Structural, Electronic, and Magnetic Properties of Gold Cluster Anions Doped with Zinc: Au_nZn^- ($2 \leq n \leq 10$)

Huai-Qian Wang,[†] Xiao-Yu Kuang,*[,†,‡] and Hui-Fang Li[†]

Institute of Atomic and Molecular Physics, Sichuan University, Chengdu 610065, China, and International Centre for Materials Physics, Academia Sinica, Shenyang 110016, China

Received: August 21, 2009; Revised Manuscript Received: October 15, 2009

The geometrical structures, relative stabilities, electronic, and magnetic properties of zinc-doped gold cluster anions Au_nZn^- ($2 \leq n \leq 10$) have been systematically investigated by means of first-principles density functional calculations at the B3LYP level. The results show that the most stable isomers have a planar structure and resemble pure gold cluster anions in shape, and no 3D isomers were obtained. Calculated dissociation energy, the second difference energy, and the highest occupied−lowest unoccupied molecular orbital gaps as a function of the cluster size exhibit a pronounced even−odd alternation phenomenon. The first vertical detachment energy of the anion clusters were calculated and compared with available experimental results. A good agreement between experimental and theoretical results suggests good prediction of the lowest-energy structures for all clusters calculated in the present study. Furthermore, both the local and total magnetic moments display a pronounced odd−even oscillation with the number of gold atoms.

I. Introduction

In recent years, an added interest in the area of the physical and chemical properties of gold and doped gold clusters is created by their potential technological applications for the fabrication of materials in nanotechnology,[1−9] materials science,[10,11] catalysis,[12−15] biology,[16−18] and medicine.[19] In light of the experimental and theoretical investigations on structural and electronic properties of neutral and charged gold clusters, the substantial debate has been already generated especially in the size regime of planar to 3D structural transformation. Ion mobility measurements combined with DFT calculations predicted that the transition of neutral gold clusters from 2D to 3D at $n = 15$,[20] whereas the cationic gold clusters are planar up to $n = 7$,[21] and gold cluster anions up to $n = 12$.[22] However, Häkkinen et al. showed that neutral and anionic gold clusters favor 2D structures up to $n = 13$.[23,24] These different viewpoints above opened up more interesting possibilities of gold clusters.

Apart from pure clusters, there are many studies of doped clusters containing gold atoms. Tanaka et al.[25−27] carried out a series of density functional investigations on neutral and cationic Au_nZn clusters and studied the structure and bonding of the bimetallic Au_5Zn^+ cluster to elucidate an anomalous stability of this cluster in the abundance of Au_nZn^+ ($n = 2-44$) clusters measured with cationic fragmentation mass spectrometry.[26,27] It should be pointed out that the Au_5Zn^+ cluster can be regarded as a σ aromatic bimetallic cluster with six delocalized s electrons.[27] They also predicted that all of the lowest-energy isomers of Au_nZn ($n \leq 6$) clusters and their cations are 2D structures very similar to those of pure Au clusters.[25] In comparison to neutral and cationic Au_nZn clusters, almost nothing is known about the Au_nZn cluster anions. Although an anion photoelectron spectroscopy measure for anionic Au_nZn clusters has been performed by Koyasu et al.,[28] and Wang et al. also determined the electronic and structural properties of the doped clusters MAu_{16}^- (M = Ag, Zn, In),[29] there is no systematic theoretical investigation on the bimetallic Au_nZn^- ($2 \leq n \leq 10$) clusters until now. The functions of bonding and valence are still unknown. Whether their structures and properties differ from those of the bare gold clusters greatly? So there is an urgent need to understand structures, electronic, and magnetic properties in small gold cluster anions doped with zinc.

In the current work, we investigate the doping of the golden cluster anions by zinc metal atom, bimetallic Au_nZn^- ($2 \leq n \leq 10$) clusters, using the first principles method on the basis of DFT. Effective core potentials (ECP) including relativistic effects for the gold and zinc atoms (RECP) are introduced to describe the inner-core electrons. The stable geometrical structures with their electronic states, relative stabilities, and electronic and magnetic properties of zinc-doped gold clusters Au_nZn^- ($2 \leq n \leq 10$) will be investigated systematically. All of the structures reported here have positive vibrational frequencies toward the nuclear displacements and therefore correspond to the potential energy minima. It is hoped that this work would be useful to understand the influence of material structure on its properties and could offer relevant information for further experimental and theoretical studies. This article is organized as follows: Section II gives a brief description of the theoretical approach. The geometrical structures, relative stabilities, electronic, and magnetic properties of zinc-doped gold clusters Au_nZn^- ($2 \leq n \leq 10$) are given in Section III, and Conclusions are summarized in section IV.

II. Theoretical Methods and Computational Details

DFT methods, which attempt to include electron correlation effects, have been widely described to be a practical and effective computational tool, especially for metallic clusters. Among DFT procedures, the most reliable approximation is often thought to be the hybrid Hartree−Fock (HF)/DFT method using a combination of the Becke's three-parameter hybrid functional incorporating the Lee−Yang−Parr correlation functional known as B3LYP,[30−32] which has been used successfully

* To whom correspondence should be addressed. E-mail: scukxy@163.com.
† Sichuan University.
‡ Academia Sinica.

10.1021/jp908084u
Published on Web 10/29/2009

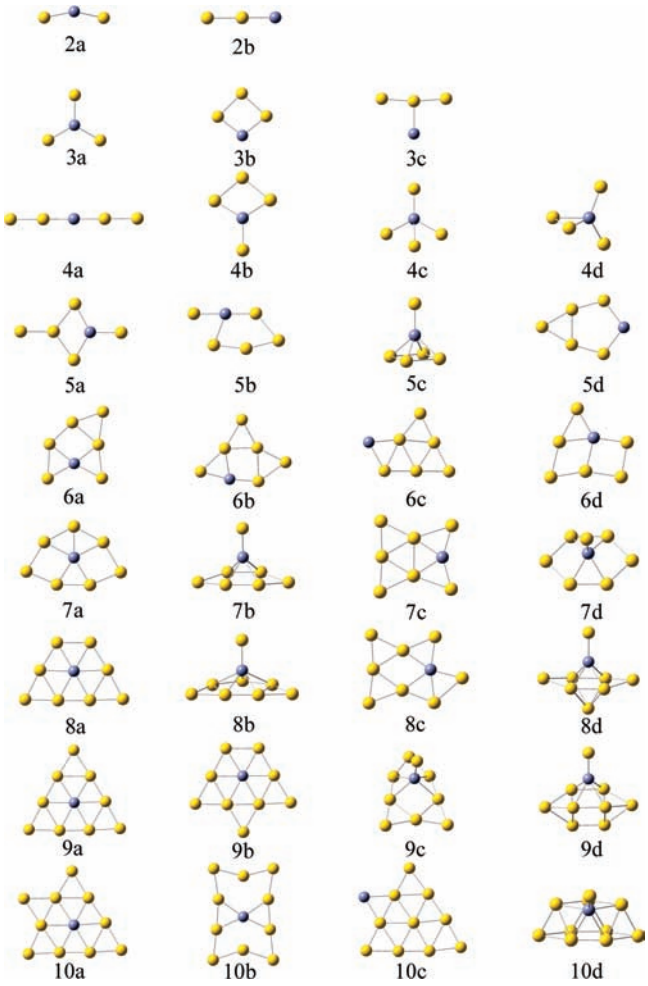

Figure 1. Lowest-energy structures and low-lying isomers for the Au_nZn^- ($2 \le n \le 10$)clusters. The yellow and blue balls represent Au and Zn atoms, respectively.

for metallic clusters based on the recent literature.[25,33] All calculations were performed with the *GAUSSIAN 03* program.[34] In present calculations, full electron calculation for the Au_nZn^- clusters anions is rather time-consuming, so it is better to introduce effective core potentials including relativistic effects (RECP) for the Au and Zn atoms to describe the inner-core electrons. Under this approximation, the $5s^25p^65d^{10}6s^1$ outermost valence electrons of the Au atom and $3s^23p^63d^{10}4s^2$ outermost valence electrons of the Zn atom are described through the corresponding LanL2DZ basis sets.[35−37] In this article, for each cluster size, although a large number of possible initial isomers for Au_nZn^- ($2 \le n \le 10$) clusters are extensively explored, we only list a few of the low-energy isomers in Figure 1. Equilibrium geometries of Au_nZn^- clusters are optimized, and their stabilities are reassured accurately by the harmonic vibrational frequency calculation. If an imaginary vibrational mode is found, a relaxation along the coordinates of the imaginary vibrational mode is carried out until the true minimum is actually obtained. In addition, single-point energies of the corresponding neutral isomers in the anion geometries were calculated to evaluate the first vertical detachment energy (VDE) of the anion isomers. All charge populations were obtained with the natural population analysis (NPA).[38,39] The highest occupied-lowest unoccupied molecular orbital (HOMO−LUMO) gaps of the most stable isomers of Au_nZn^- ($2 \le n \le 10$) were also obtained from B3LYP method with the LanL2DZ effective core potential and basis set.

TABLE 1: Geometries, Symmetries, Electron State, and Relative Energies ΔE (in eV) of Au_nZn^- ($2 \le n \le 10$) Clusters

	sym	state	ΔE		sym	state	ΔE
2a	C_{2v}	$^2A_1$	0	7a	C_s	$^1A'$	0
2b	$C_{\infty v}$	$^2\Sigma^+$	0.39	7b	C_{2v}	$^1A_1$	0.0003
3a	C_{2v}	$^1A_1$	0	7c	C_s	$^1A'$	0.19
3b	C_{2v}	$^1A_1$	0.73	7d	C_{2v}	$^3A_1$	1.12
3c	C_{2v}	$^1A_1$	0.76	8a	C_s	$^2A'$	0
4a	$D_{\infty h}$	$^2\Sigma_u$	0	8b	C_s	$^2A'$	0.39
4b	C_{2v}	$^2A'_1$	0.05	8c	C_s	$^2A'$	0.46
4c	C_s	$^2A'$	0.05	8d	C_s	$^2A'$	0.93
4d	C_1	$^2A_1$	0.10	9a	C_s	$^1A'$	0
5a	C_s	$^1A'$	0	9b	C_s	$^1A'$	0.63
5b	C_s	$^1A'$	0.02	9c	C_s	$^1A'$	0.70
5c	C_1	$^1A_1$	0.18	9d	C_s	$^1A'$	1.36
5d	C_s	$^1A'$	0.65	10a	C_{2v}	$^2A_1$	0
6a	C_1	^2A	0	10b	C_{2v}	$^2A_1$	0.29
6b	C_s	$^2A'$	0.11	10c	C_{2v}	$^2A_1$	0.66
6c	C_s	$^2A'$	0.54	10d	C_1	^2A	1.15
6d	C_s	$^4A'$	1.11				

To predict relative stabilities of Au_nZn^- ($2 \le n \le 10$) clusters, we have calculated the binding energy per atom [$E_b(n)$], dissociation energy [$\Delta_1E(n)$], and the second difference energy [$\Delta_2E(n)$], which are defined as following formula:[45]

$$E_b(n) = \frac{E(Zn^-) + nE(Au) - E(Au_nZn^-)}{n+1} \quad (1)$$

$$\Delta_1E(n) = E(Au_{n-1}Zn^-) + E(Au) - E(Au_nZn^-) \quad (2)$$

$$\Delta_2E(n) = E(Au_{n-1}Zn^-) + E(Au_{n+1}Zn^-) - 2E(Au_nZn^-) \quad (3)$$

where $E(Zn^-)$, $E(Au)$, $E(Au_nZn^-)$, $E(Au_{n-1}Zn^-)$, and $E(Au_{n+1}Zn^-)$represent the total energies of the most stable Zn^-, Au, Au_nZn^-, $Au_{n-1}Zn^-$, and $Au_{n+1}Zn^-$ clusters, respectively. It is worth pointing out that all of the clusters are found to prefer the lowest spin state.

III. Results and Discussion

A. Low-Energy Structures and Vertical Detachment Energies. A number of optimized low-lying structures for Au_nZn^- ($2 \le n \le 10$) clusters are shown in Figure 1 and their corresponding relative energies, symmetries, and electron state are summarized in Table 1. According to the total energy from low to high, the low-lying isomers are designated by na, nb, nc, and nd, n is the number of Au atoms. It must be pointed out that a large number of initial structural candidates were considered but here we report only the few energetically lowest-lying isomers for each size.

The calculated results for $AuZn^-$ show that the singlet spin state is lower in energy than the triplet and quintet spin states by 2 and 5.88 eV, respectively. Equilibrium bond distances of $AuZn^-$ are calculated to be as long as 2.765 Å, which is longer than that of neutral (2.515 Å) and cationic (2.407 Å) AuZn. Furthermore, the calculated bond energy of the anion (0.65 eV) is smaller than that of neutral (0.99 eV) and cation (2.73 eV) calculated for the dissociation to the Au, Zn and Au, Zn^+ cation,[25] indicating that the Au−Zn^+ bond is stronger than the Au^-−Zn and Au−Zn bonds.

The possible Au_2Zn^- clusters with different spin electronic configurations considered are optimized. In our calculations, we find the lowest-energy isomer, 2a (Figure 1), is a planar structure and has C_{2v} symmetry with an apex angle of 156.6°. The isosceles triangle 2a isomer with electronic state of $^2A_1$ is the ground-state structure, which is energetically lower than the same structure with other spin states. Its VDE is calculated as 1.70 eV, which is in good agreement with the available experimental data [1.68 ± 0.03 (ref 28)]. The energetically closest isomer (structure 2b) is a doublet state ($^2\Sigma^+$) with $C_{\infty v}$ symmetry, and it is 0.39 eV higher in energy than 2a. It is notable that Au_2Zn^- has triangular isomer (2a) unlike $Au_2Zn^{+,0}$ calculated by Tanaka et al.[25] The triangularity of the Au_2Zn^- is found to be due to an extra bond formed by overlap between a vacant 4p orbital of Zn and valence 6s (5d) orbital of Au; meanwhile, the triangle structures can increase the Au−Au bond interaction so as to obtain the lowest-energy structures. To explain the geometric characteristics onward, we examine the compositions of their highest occupied molecular orbital (HOMO) further: for 2a isomer, HOMO in α-spin (up) and β-spin (down) are contributed from Au6*s* (63.9% for spin α, 96.8% for spin β), Zn4s (26.5% for spin α) and Zn4p (2.6% for spin β).

In the calculations, we find three different isomers within an energy range of 0.76 eV. The lowest-energy Y-shaped isomer 3a, which becomes a Zn-centered Au_3triangle, is planar structure with C_{2v} symmetry. This Y-shaped structure has been found in ref 25 for the Au_3Zn cluster, and the calculated results show that the singlet ($^1A_1$) 3*a* isomer with a bond length of 2.538 Å is lower in total energy than the 3b and 3c isomers by 0.73 and 0.76 eV respectively, indicating that the 3*a* is more stable than other isomers. The geometry of rhombus isomer 3b was found as the ground state of both neutral and cationic Au_4 clusters in the article by E. M. Fernández and co-workers.[40] Rhombus isomer 3b is energetically less favorable than the Y-shaped structure because the square shape forces Au−Zn bond distances to be longer. T-shaped isomer 3c and rhombus isomer 3b have almost the same energies. Interestingly, three isomers 3a, 3b, 3c, have the same symmetries (C_{2v}) and electronic state $^1A_1$ (Table 1), whereas isomers 3a has the biggest VDE as will be discussed in detail in section C. The rhombus 3b isomer resembles the lowest energy structure of Au_4.[41−43] To understand the contribution of doped Zn atom on the HOMO onward, we examined the compositions of HOMO for 3a: 91.3% of Au 6s and 3.1% of Zn 4p. The significant s orbital character of Au atom in the frontier orbitals is found. The unique s−p interaction between gold and impurity atoms would impact the geometrical structures and stability of Zn-doped gold clusters.

Four isomers for Au_4Zn^- were found in the present calculation. Surprisingly, the lowest-energy isomer 4a has a linear $D_{\infty h}$ symmetry, and this situation is ambiguous when considering the VDE: the experimental data is 2.67 ± 0.02 eV;[28] however, structure 4a has a calculated value of 3.36 eV! Again we performed an extensive search for other isomers. In our subsequent search for the global minimum, we find two planar structures (4b, 4c) to be lowest in energy and almost degenerate (0.05 eV, 0.05 eV; Table 1), whereas calculated VDE values (2.62 eV, 2.60 eV) are in line with experimental data (2.67 ± 0.02 eV). However, why one finds this disagreement in VDE values for the most stable structure, and why one isomer which is not the most stable has a much better VDE correlation with the experimental value? On the one hand, only 0.05 eV above the linear isomer (4a) is a scoop-shaped structure (4b) with a VDE of 2.62 eV. On the other hand, this energy difference is clearly smaller than the error inherent in the computational method, which we estimate to be about 0.05−0.1 eV in this size range. The lowest 3D isomer 4d with C_1symmetry is 0.10 eV less stable than the planar isomer 4b. Its VDE is 3.44 eV, clearly bigger than the experimental value. 4d is the smallest 3D isomeric structure of Au_4Zn^- clusters found in the present calculation. Therefore, 4b isomer is our most proper structure.

Theoretical calculations indicated that the enhanced stability of Au_5Zn^+ can be regarded as a σ aromatic bimetallic cluster with six delocalized s electrons.[26,27] Tanaka et al. pointed out that the lowest-energy isomer Au_5Zn^+ with C_{2v} symmetry has a triangular structure in which the Zn atom locates on a side of the triangle. Using this information as a guide, the calculation again predicts planar structures to be lowest in energy; the two lowest 5a and 5b (0.02 eV) isomers are almost degenerate. The calculated VDE value is 3.69 eV for isomer 5a, in line with the experimental value of 3.64 ± 0.02 eV. We also find another deformed planar 5d with C_s symmetry, within 0.65 eV. Its VDE is 3.08 eV, clearly smaller than the experimental value. Furthermore, we have not found any low-lying 3D structures: the lowest 3D structure we find is a trigonal pyramid 5c.

With regard to the Au_6Zn^- cluster, the calculation again predicts planar structures to be lowest in energy; the two lowest 6a and 6b (0.11 eV) are almost degenerate. We find two other structures 6c, 6d within 1.11 eV of the lowest. The lowest-energy structure (6a) we find is lowly symmetrical and planar: it is a deformed planar with C_1 symmetry, which resembles the lowest-energy structure of neutral Au_6Zn cluster.[25] The 6b isomer, which is 0.11 eV higher in energy than the 6a isomer, possesses a planar C_s symmetry structure. The planar structures (6a, 6b) are obtained by replacing one Au atom on the center sites by impurity Zn atom for Au_7^-.[22,40] The experimental VDE value is 2.56 ± 0.02 eV; isomer 6a has a calculated value of 2.61 eV, isomer 6b of 2.64 eV, isomer 6c of 2.66 eV, isomer 6d of 2.52 eV. Furthermore, it is noteworthy that no 3D isomers were found for the Au_6Zn^- cluster.

In the case of Au_7Zn^-, according to our calculations the lowest-energy structure is also planar. The two lowest 7a and 7b (0.0003 eV) are almost degenerate. The planar structure 7a with electronic state of $^1A'$ is obtained by replacing one center Au atom in the second most stable pure Au_8^- isomer,[22] its VDE is 3.40 eV, in reasonable agreement with experiment (3.38 ± 0.02, Table 1). The lowest 3D isomer 7b with C_{2v} symmetry is only 0.0003 eV less stable than the planar isomer 7a. Its VDE is 3.79 eV, clearly bigger than the experimental value. Again, we performed an extensive search for other isomers. The next higher structure we found 7c and 7d are energetically higher than the 7a isomer by 0.19 and 1.12 eV, respectively. The 7c isomer shows a similar structure to the third isomer of Au_7M (M = Ni, Pd, Pt)[44] and the ground state of the Au_8^-[40] cluster. 7b and 7d isomers have the same hexagonal pyramidal 3D structure but their relative energy is different a lot (1.12 eV), for one thing the spin multiplicity of 7b is lower than 7d (Table 1), for another the average nearest-neighbor distance of 7b (2.67 Å) is shorter than 7d (2.69 Å).

For n = 8, the lowest-energy isomer 8a has a planar trapeziform structure with electronic state of $^2A'$, and it is obtained by replacing one center Au atom in the most stable pure Au_9^- isomer.[1,22,40] The structure 8a coincides with that for Au_8Sc^+ and Au_8Ti^+ obtained by M. B. Torres and co-workers.[43] We find three other structures 8b, 8c, 8d within 0.93 eV of the lowest. Isomer 8b has a heptagonal pyramidal 3D structure, and it is 0.39 eV less stable than the 8a isomer. The structure 8c (C_s symmetry) is based on a four-star shape 7c isomer. The 8d

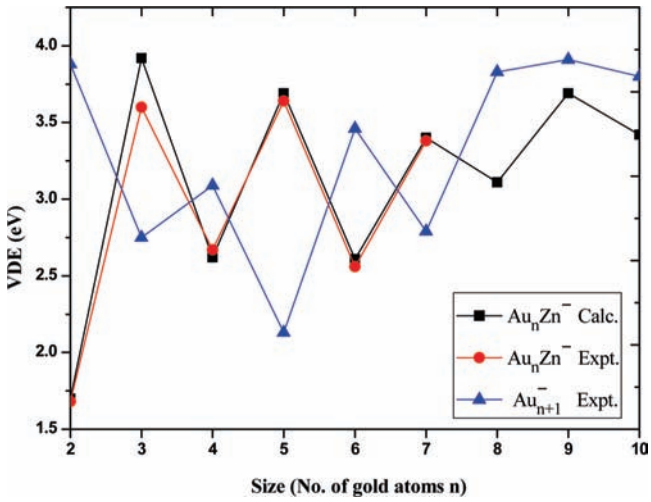

Figure 2. Calculated and experimentally measured (ref 28) vertical electron detachment energies (VDE) as a function of clusters size.

isomer has a hexagonal bipyramid 3D structure with C_s symmetry, and it is 0.93 eV higher in energy than the 8a isomer. Calculated VDE values for isomers 8a−8d are 3.11 eV, 3.43 eV, 3.01 eV, 3.33 eV, respectively. Unfortunately there are no experimental data of VDE so far, our calculated results are significantly smaller than Au_9^- isomer (3.83 eV).[1]

According to our calculations, the lowest-energy structure of Au_9Zn^- is also planar. We found four C_s symmetric lowest-energy structures: planar triangle with the impurity Zn atom located at the center sites in our calculations for 9a isomer, which can be derived from the pure Au_{10}^- cluster;[1,22,40] planar isomer 9b can be obtained by adding an Au atom to trapeziform structure 8a, is less stable than 9a isomer by 0.63 eV; the kite-shaped 9c and sailboat-shaped 9d isomers are less stable than 9a isomer by 0.70 and 1.36 eV, respectively. The experimental VDE value is 3.91 ± 0.02 eV for Au_{10}^- clusters,[1] isomer 9a has a calculated value of 3.69 eV, isomer 9b of 3.64 eV, isomer 9c of 3.86 eV, isomer 9d of 3.90 eV.

For $Au_{10}Zn^-$ clusters, the calculation again predicts planar structures to be lowest in energy; three high symmetric lowest-energy structures 10a, 10b, 10c within 0.66 eV of the lowest. We consider that the high symmetric structures are determined by the high symmetry of the pure host gold cluster Au_{11}^-.[22,23] Planar 10a and 10b isomers with the impurity atom located at the center sites in our calculations, which are obtained by replacing one Au atom on the center sites by impurity Zn atom for the second and third stable structures (Au_{11}^-).[1,22]

Calculated and experimentally measured (ref 28) VDE as a function of clusters size is plotted in Figure 2. From Figure 2, we can see that our VDE results are all appreciably underestimated but the trend is in good agreement with the experimental results.[28] The calculated VDE values of the ground-state structures 2a (1.70 eV), 3a (3.92 eV), 4b (2.62 eV), 5a (3.69 eV), 6a (2.61 eV), and 7a (3.40 eV) agree reasonably well with the experimental values of 1.68, 3.60, 2.67, 3.64, 2.56, 3.38 eV, respectively. It should be pointed that the experimental VDE of the 5a and 7a isomers match the very weak photoelectron spectroscopy (PES) feature at 2.40, 2.81 eV, the first VDE should be 3.64, 3.38 eV, respectively. It can be seen from Figure 2 that the remarkably good agreement between the calculated VDE values and the measured ones, and the largest relative deviation, ~8.9%, occurring for Au_3Zn^-. To find the reason for the large deviation between the theory and experiment, we try to use other methods to calculate the VDE values for 3a isomer. The first DFT method is B3LYP method and the second functional is BP86 method. These two functionals are the popular method and have been shown to be effective tool for the investigation of metallic clusters. We adopt the same basis set for the Au_3Zn^- cluster as that in the study of the Au_nZn ($n \le 6$) clusters and their cations.[25] For the Zn atom, the Wachter-Hay all electron basis set (the 6-311+G* basis set) is used. For the Au atom, LanL2DZ is used. The geometry of the 3a isomer is optimized using the two DFT methods and the VDE values are determined. The calculated value of VDE is 4.35 eV by BP86, which is clearly larger than the experimental value. The VDE value is 3.91 eV by B3LYP method, which is essentially consistent with the result in this work. Unfortunately, there are no experimental data of VDE for $n \ge 8$ until now, however, there is no obvious relationship between the values for Au_nZn^- and pure Au_{n+1}^- clusters, as can be seen in Figure 2. Our calculated results for ground-state structures 8a (3.11 eV), 9a (3.69 eV), 10a (3.42 eV) are significantly smaller than pure Au_9^- (3.83 eV), Au_{10}^- (3.91 eV), Au_{11}^- (3.80 eV) isomers,[1] respectively. The anticorrelation shown in Figure 2 between the VDE of Au_nZn^- and Au_{n+1}^- clusters is due to the typical odd−even electronic effect: Au_nZn^- clusters have one electron more than Au_{n+1}^-clusters.

According to the above discussion on the Au_nZn^- ($2 \le n \le 10$) clusters, the most stable planar structures are found to prefer the lowest spin state; however, no 3D lowest-energy structure is found though by adopting stable structures of pure gold and alkali metal clusters as an initial structure but all of the attempts failed in the present study.

B. Relative Stability. The calculated the binding energy per atom, dissociation energy, and the second difference energy for the most stable Au_nZn^- isomers as a function of clusters size are plotted in parts a−c of Figure 3. The curves of results show that Au_3Zn^- is most stable and the cluster stability has an odd−even alternation phenomenon along with cluster size. Part a of Figure 3 presents the binding energy per atom for the ground state as a function of cluster size. As seen from part a of Figure 3, the local peaks of the atomic averaged binding energies for the lowest-energy clusters localize at $n = 3$, 5, and 9, indicating that these clusters are more stable than their neighboring clusters. Furthermore, the dissociation energy [$\Delta_1 E(n)$] and the second difference energy [$\Delta_2 E(n)$] are sensitive indicators of the relative stability. Parts b and c of Figure 3 show the dissociation energy and the second difference energy of anions of doped gold clusters as a function of cluster size. The atomic dissociation energies and second differences of energies of Au_nZn^- ($2 \le n \le 10$) clusters exhibit pronounced even−odd alternations, which indicates that the clusters, with even valence electrons (3a, 5a 7a, and 9a), keep higher stability compared with their vicinity clusters. According to parts a−c of Figure 3, it shows apparently that the maximum magic number of the relative stability is $n = 3$ among investigated Au_nZn^- ($2 \le n \le 10$) clusters, reflecting that the Au_3Zn^- cluster is the most stable geometry, which is in good agreement with the anion photoelectron spectroscopy.[28]

The especial stability of Au_3Zn^- cluster is due to the magic character of planar metallic clusters with 6 valence electrons.[25,26,40] The Au_3Zn^- cluster can be seen as the building block of the novel material because of its large relative stability and strong chemical stability which is discussed below.

C. Electronic Properties. The electronic properties of Au_nZn^- clusters are discussed by examining the energy gap between the HOMO and LUMO. The HOMO−LUMO energy gap reflects the ability for electrons to jump from occupied orbital

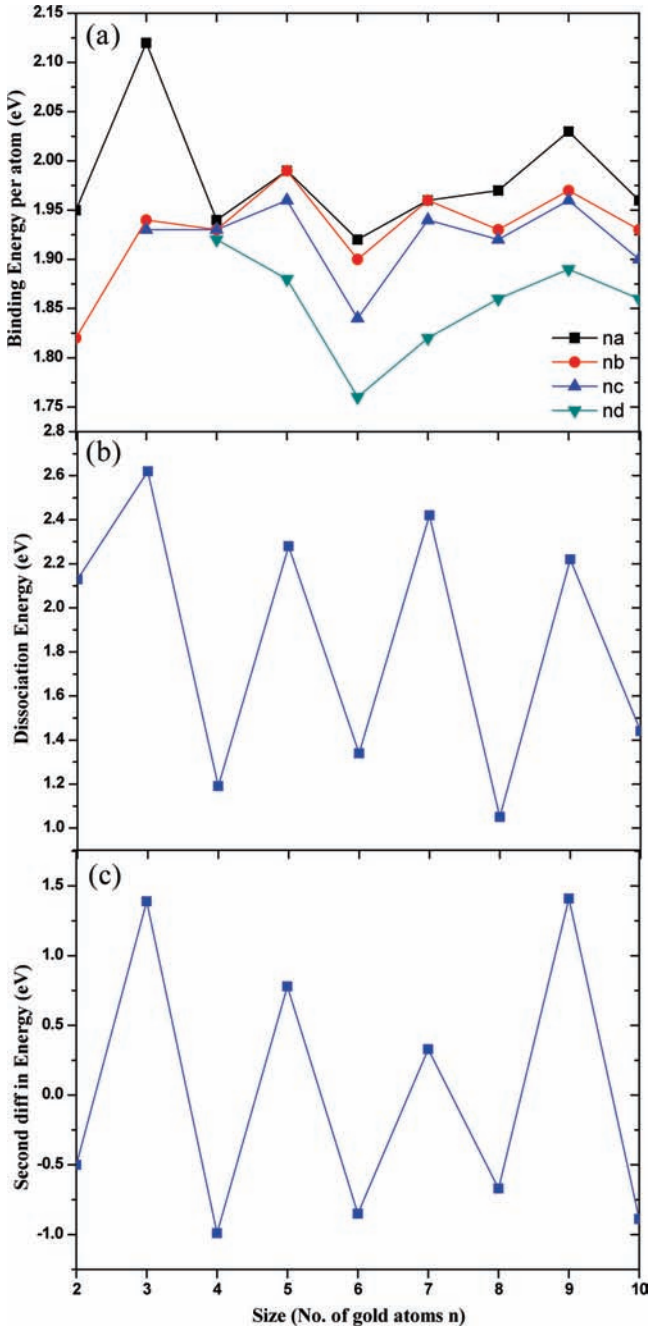

Figure 3. (a) Binding energies per atom for a−d Au_nZn^- isomers as a function of clusters size. Size dependence of dissociation energies (b) and the second difference of energies (c) for the lowest-energy structure of Au_nZn^- clusters.

to unoccupied orbital and represents the ability for the molecular participates to produce chemical reactions to some degree. A large gap corresponds to a high strength required to perturb the electronic structure, namely a bigger gap indicates a weaker chemical activity. For open-shell systems, the HOMO is single occupied and can easily accept or lose electron; the respective gap is zero by definition. This zero gap will happen for all clusters Au_nZn^- with even n. The HOMO−LUMO energy gap for the most stable geometry at each cluster size is shown in Figure 4. As seen from Figure 4, the primary features are concluded below: (a) the HOMO−LUMO gaps for the most stable Au_nZn^- ($2 \le n \le 10$) clusters range from 0 to 3.26 eV, (b)Au_3Zn^- has the largest HOMO−LUMO gap of 3.26 eV, and (c) it is interesting to note that HOMO-LUMO gaps exhibit

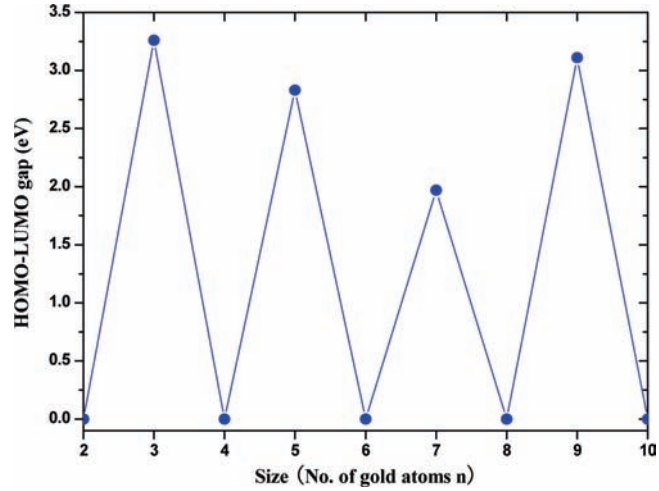

Figure 4. Size dependence of the HOMO−LUMO gaps for the lowest-energy structure of Au_nZn^- clusters.

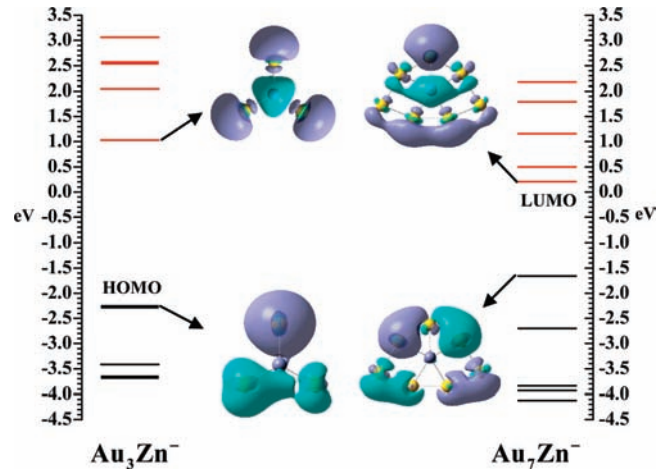

Figure 5. Calculated molecular orbital energy levels of Au_3Zn^- and Au_7Zn^- clusters together with the molecular orbital maps of the HOMOs and LUMOs. Green and red correspond to the different phases of the molecular wave functions for the HOMOs and LUMOs, and the isovalue is 0.02 au.

odd−even oscillations, indicating that odd-numbered Au_nZn^- clusters are relatively more stable than the neighboring even-numbered sizes. The HOMO−LUMO gap is particularly large for Au_3Zn^-, Au_5Zn^-, Au_7Zn^-, and Au_9Zn^- (3.26, 2.83, 1.77, and 3.11 eV, respectively), which accords with the behavior of the second difference in energy $\Delta_2E(n)$ and dissociation energy $\Delta_1E(n)$ (parts b and c of Figures 3). (d) We also note that Au_3Zn^- has the largest HOMO−LUMO gap of 3.26 eV, indicating that the Au_3Zn^- cluster has dramatically enhanced chemical stability.

In light of the particular phenomenon where the gap of Au_3Zn^- cluster is the largest (3.26 eV) but the gap of Au_7Zn^- is the smallest (1.77 eV) in Au_nZn^- clusters (with odd n), the energy levels of molecular orbital for Au_3Zn^- and Au_7Zn^- are displayed in Figure 5. The black line shows the occupied orbitals and the red line shows the unoccupied orbitals. Compared with Au_3Zn^- and Au_7Zn^-, Au_3Zn^- obviously is characteristic of the molecular orbital producing the degeneration of the energy level in the vicinity of the HOMO−LUMO and the energy level of the LUMO elevated strongly, which probably leads to its largest value of energy gap. Furthermore, our natural population analysis (NPA) results for the lowest energy Au_nZn^- species are summarized in Table 2. NPA clearly shows the ionic

TABLE 2: Natural Charges Populations of the Lowest-Energy Au_nZn^- ($2 \le n \le 10$) Clusters

n	Zn	Au-1	Au-2	Au-3	Au-4	Au-5	Au-6	Au-7	Au-8	Au-9	Au-10
2	0.250	−0.625[a]	−0.625[a]								
3	0.295	−0.432[a]	−0.431[a]	−0.431[a]							
4	0.249	−0.298[a]	−0.296[a]	−0.388[a]	−0.268						
5	0.261	−0.291	−0.183[a]	−0.348[a]	−0.182[a]	−0.256					
6	0.317	−0.241	−0.134	−0.227[a]	−0.168[a]	−0.247[a]	−0.300[a]				
7	0.412	−0.159[a]	−0.259	−0.247[a]	−0.156[a]	−0.247[a]	−0.083[a]	−0.262			
8	0.430	−0.200[a]	−0.174	−0.181[a]	−0.160[a]	−0.175	−0.181[a]	−0.197[a]	−0.161[a]		
9	0.534	−0.181	−0.168[a]	−0.159[a]	−0.165[a]	−0.184	−0.168[a]	−0.164[a]	−0.163[a]	−0.183	
10	0.584	−0.185	−0.146[a]	−0.146[a]	−0.156[a]	−0.108	−0.156[a]	−0.277[a]	−0.277[a]	−0.108	−0.027

[a] Atoms bonding to Zn atom.

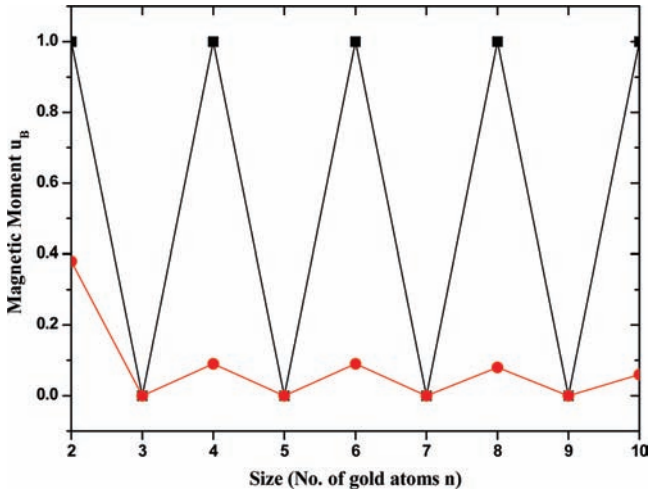

Figure 6. Total magnetic moment of the Au_nZn^- ($2 \le n \le 10$) clusters (solid squares) and local magnetic moment on the Zn atom (solid dots).

character of the Zn−Au bond in these clusters, in which the Zn atom attracts 0.249−0.584e charges from its neighboring Au atoms. The charge distribution is dependent on the symmetry of the cluster. We also checked natural bond orbital. The calculated nonorthogonal natural atomic overlap populations between Au and Au are larger than those between Au and Zn. It might be expected that Au−Au interactions are largely responsible for the larger stability of Au_nZn^- clusters. To compare the degree of electron delocalization in the anionic clusters, the number of valence s electrons assigned on each atom in the different isomers is obtained by NPA. The electrons occupying vacant 4p orbital of Zn are not included in the number of s electrons count, which is shown in Table 2. Au_nZn^- ($2 \le n \le 10$) clusters, in which s electrons delocalize over all atoms as equally as possible, tend to be favorable structures for almost all the clusters. Take Au_3Zn^- for example, the NPA results on Au_3Zn^- indicate that there are about 0.7 electrons transferred from s valence orbital of Zn atom to the p valence orbital. The NPA result supports the adequacy of the electronic shell model applied for the doped Au clusters[46] because this model assumed that a valence electron moves freely in an averaged potential provided by the ionic core and the other electrons. The larger cluster sizes, the more assigned electrons for s electrons in the ground state electronic configuration of Au and Zn atoms.

D. Magnetic Properties. On the basis of the most stable geometries, the total magnetic moments of Au_nZn^- ($2 \le n \le 10$) as well as the local magnetic moments of Zn atoms in Au_nZn^- clusters were presented in Figure 6. As seen from Figure 6, the total magnetic moments of Au_nZn^- as a function of the cluster size show a dramatic odd−even alternative behavior, indicating that, for the Au_nZn^- clusters with even n, the total magnetic moment is μ_B, whereas for odd n, the value is zero. The trend of the magnetic moment is in agreement with the results of NiB_n.47 The total magnetic moment is mainly located on the Au atoms, whereas the magnetic moment located on the Zn atoms is small about 0.06−0.38 μ_B.

TABLE 3: Charge and Magnetic Moment of 3d, 4s, and 4p States for the Zn Atom in Au_nZn^- ($2 \le n \le 10$) Cluster

	Zn-3d		Zn-4s		Zn-4p	
cluster	$Q(e)$	$\mu(\mu_B)$	$Q(e)$	$\mu(\mu_B)$	$Q(e)$	$\mu(\mu_B)$
Au_2Zn^-	9.99	0	1.46	0.38	0.30	0
Au_3Zn^-	9.99	0	1.01	0	0.70	0
Au_4Zn^-	9.99	0	1.02	0.10	0.73	−0.01
Au_5Zn^-	9.98	0	0.95	0	0.80	0
Au_6Zn^-	9.98	0	0.90	0.06	0.79	0.03
Au_7Zn^-	9.98	0	0.76	0	0.84	0
Au_8Zn^-	9.98	0	0.83	0.09	0.75	−0.01
Au_9Zn^-	9.98	0	0.80	0	0.67	0
$Au_{10}Zn^-$	9.98	0	0.82	0.02	0.60	0.04

To further understand the magnetic properties of Au_nZn^- ($2 \le n \le 10$) clusters, we performed a detailed analysis of the onsite atomic charges and local magnetic moment of Zn atom in Au_nZn^- clusters. The charges of 3d, 4s, and 4p states for the Zn atom in Au_nZn^- clusters are summarized in Table 3. Table 3 shows that the magnetic moment of the Zn atom is mainly from the 4s state except for $Au_{10}Zn^-$, following is the 4p state and the 3d state without contributing to the magnetic moment of the Zn atom. For free Zn and Au atoms, the configuration of valence electrons is $3d^{10}4s^2$ and $5d^{10}6s^1$, respectively. When the Zn and Au atoms combine to form the Au_nZn^- ($2 \le n \le 10$) clusters, the configuration of valence electrons is $3d^x4s^y4p^z$ ($9.98 \le x \le 9.99$, $0.82 \le y \le 1.46$, $0.30 \le z \le 0.84$) for the Zn atom and $5d^{x'}6s^{y'}6p^{z'}$ ($9.90 \le x' \le 9.95$, $0.84 \le y' \le 1.61$, $0.01 \le z' \le 0.42$) for Au atoms, obviously, 4s state lose electrons, meanwhile, the 4p state of Zn gains some amount of electrons. Namely, there is internal electron transfer from 4s state to the 4p state in the Zn atom. Thus, for the Au_nZn^- clusters, the charge transfer mainly happens between Zn 4s and 4p and Au 6s and 6p states. Furthermore, it can be seen from Figure 6 that the local magnetic moments of Zn atom also show pronounced odd−even alternative phenomenon and are oscillatory decreased ranging from 0.38 to 0.06 with increasing cluster size.

IV. Conclusions

The geometrical structures, relative stabilities, and electronic and magnetic properties of zinc-doped gold clusters Au_nZn^- ($2 \le n \le 10$) are investigated systematically at the B3LYP level employing LanL2DZ effective core potential and basis set, together with the vibrational frequency analysis. All of the results are summarized in the following:

(i) The calculations revealed that all of the lowest-energy isomers of Au_nZn^- ($2 \le n \le 10$) clusters are 2D structures very

similar to those of the pure gold cluster anions as well as neutral and cationic Au_nZn ($n \leq 6$) clusters.

(ii) The dissociation energy, the second difference energy, and the HOMO−LUMO gaps of the most stable Au_nZn^- ($2 \leq n \leq 10$) clusters exhibit an interesting, oscillatory behavior as a function of cluster size, indicating that the clusters Au_3Zn^-, Au_5Zn^-, Au_7Zn^-, and Au_9Zn^- keep higher stability compared with their vicinity clusters. Especially for the Au_3Zn^- cluster shows the strongest stability due to its local peak of all the curves (Figure 2 and parts a and b of Figure 3) of $E_b(n)$, $\Delta_1E(n)$, and $\Delta_2E(n)$. Furthermore, the largest value of energy gap (3.26 eV) for Au_3Zn^- probably results from the molecular orbital producing the degeneration of the energy level in the vicinity of the HOMO−LUMO and the energy level of the LUMO elevated strongly.

(iii) The local magnetic moment of the doped zinc atom shows a pronounced odd−even oscillation with the number of Au atoms and decreases when the cluster size increases. It must be pointed that the ground-state Au_nZn^- ($2 \leq n \leq 10$) clusters with odd-numbered atoms have a total magnetic moment of μ_B, which is mainly located on the Au atoms (about $0.62-0.94\ \mu_B$), whereas for even-numbered atoms exhibit nonmagnetic ground states.

Acknowledgment. This work was supported by the Doctoral Education Fund of Education Ministry of China (No. 20050610011) and the National Natural science Foundation of China (No. 10774103).

Supporting Information Available: Possible initial geometries for the Au_nZn^- ($2 \leq n \leq 10$) clusters. This material is available free of charge via the Internet at http://pubs.acs.org.

References and Notes

(1) Häkkinen, H. *Chem. Soc. Rev.* **2008**, *37*, 1847.
(2) Shuford, K. L.; Meyer, K. A.; Li, C. C.; Cho, S. O.; Whitten, W. B.; Shaw, R. W. *J. Phys. Chem. A* **2009**, *113*, 4009.
(3) Qian, H. F.; Zhu, M. Z.; Andersen, U. N.; Jin, R. C. *J. Phys. Chem. A* **2009**, *113*, 4218.
(4) Nah, S.; Li, L. J.; Fourkas, J. T. *J. Phys. Chem. A* **2009**, *113*, 4416.
(5) Hu, M.; Chen, J.; Li, Z. Y.; Au, L.; Hartland, G. V.; Li, X.; Marquez, M.; Xia, Y. *Chem. Soc. Rev.* **2006**, *35*, 1084.
(6) Noonan, K. J. T.; Gillon, B. H.; Cappello, V.; Gates, D. P. *J. Am. Chem. Soc.* **2008**, *130*, 12876.
(7) Wang, T.; Hu, X. G.; Dong, S. J. *J. Phys. Chem. B* **2006**, *110*, 16930.
(8) Li, Y.; Shi, G. Q. *J. Phys. Chem. B* **2005**, *109*, 23787.
(9) Kilin, D. S.; Tsemekhman, K. L.; Kilina, S. V.; Balatsky, A. V.; Prezhdo, O. V. *J. Phys. Chem. A* **2009**, *113*, 4549.
(10) Majumder, C.; Kandalam, A. K.; Jena, P. *Phys. Rev. B* **2006**, *74*, 205437.
(11) Li, X.; Kiran, B.; Cui, L. F.; Wan, L. S. *Phys. Rev. Lett.* **2005**, *95*, 253401.
(12) Torres, M. B.; Fernández, E. M.; Balbás, L. C. *J. Phys. Chem. A* **2008**, *112*, 6678.
(13) Graciani, J.; Oviedo, J.; Sanz, J. F. *J. Phys. Chem. B* **2006**, *110*, 11600.
(14) Teles, J. H.; Brode, S.; Chabanas, M. *Angew. Chem.* **1999**, *99*, 2589.
(15) Valden, M.; Lai, X.; Goodman, D. W. *Science* **1998**, *281*, 1637.
(16) Yoon, B.; Häkkinen, H.; Landman, U.; Wörz, A. S.; Antonietti, J.-M.; Abbet, S.; Judai, K.; Heiz, U. *Science* **2005**, *307*, 403.
(17) McRae, R.; Lai, B.; Vogt, S.; Fahrni, C. J. *J. Struct. Biol.* **2006**, *155*, 22.
(18) Ackerson, C. J.; Jadzinsky, P. D.; Jensen, G. J.; Kornberg, R. D. *J. Am. Chem. Soc.* **2006**, *128*, 2635.
(19) Shaw III, C. F. *Chem. Rev.* **1999**, *99*, 2589.
(20) Xiao, L.; Wang, L. *Chem. Phys. Lett.* **2004**, *392*, 452.
(21) Gilb, S.; Weis, P.; Furche, F.; Ahrichs, R.; Kappes, M. M. *J. Chem. Phys.* **2002**, *116*, 4094.
(22) Furche, F.; Ahlrichs, R.; Weis, P.; Jacob, C.; Gilb, S.; Bierweiler, T.; Kappes, M. M. *J. Chem. Phys.* **2002**, *117*, 6982.
(23) Häkkinen, H.; Yoon, B.; Landman, U.; Li, X.; Zhai, H. J.; Wang, L. S. *J. Phys. Chem. A* **2003**, *107*, 6168.
(24) Häkkinen, H.; Moseler, M.; Landman, U. *Phys. Rev. Lett.* **2002**, *89*, 033401.
(25) Tanaka, H.; Neukermans, S.; Janssens, E.; Silverans, R. E.; Lievens, P. *J. Chem. Phys.* **2003**, *119*, 7115.
(26) Janssens, E.; Tanaka, H.; Neukermans, S.; Silverans, R. E.; Lievens, P. *New J. Phys.* **2003**, *5*, 46.
(27) Tanaka, H.; Neukermans, S.; Janssens, E.; Silverans, R. E.; Lievens, P. *J. Am. Chem. Soc.* **2003**, *125*, 2862.
(28) Koyasu, K.; Naono, Y.; Akutsu, M.; Mitsui, M.; Nakajima, A. *Chem. Phys. Lett.* **2006**, *422*, 62.
(29) Wang, L. M.; Pal, R.; Huang, W.; Zeng, X. C.; Wang, L. S. *J. Chem. Phys.* **2009**, *130*, 051101.
(30) Becke, A. D. *J. Chem. Phys.* **1993**, *98*, 5648.
(31) Lee, C.; Yang, W.; Parr, R. G. *Phys. Rev. B* **1988**, *37*, 785.
(32) Mielich, B.; Savin, A.; Stoll, H.; Preuss, H. *Chem. Phys. Lett.* **1989**, *157*, 200.
(33) Wu, Z. J. *Chem. Phys. Lett.* **2005**, *406*, 24.
(34) Frisch, M. J.; Trucks, G. W.; Schlegel, H. B.; Scuseria, G. E.; Robb, M. A.; Cheeseman, J. R.; Montgomery, Jr., J. A.; Vreven, T.; Kudin, K. N.; Burant, J. C.; Millam, J. M.; Iyengar, S. S.; Tomasi, J.; Barone, V.; Mennucci, B.; Cossi, M.; Scalmani, G.; Rega, N.; Petersson, G. A.; Nakatsuji, H.; Hada, M.; Ehara, M.; Toyota, K.; Fukuda, R.; Hasegawa, J.; Ishida, M.; Nakajima, T.; Honda, Y.; Kitao, O.; Nakai, H.; Klene, M.; Li, X.; Knox, J. E.; Hratchian, H. P.; Cross, J. B.; Bakken, V.; Adamo, C.; Jaramillo, J.; Gomperts, R.; Stratmann, R. E.; Yazyev, O.; Austin, A. J.; Cammi, R.; Pomelli, C.; Ochterski, J. W.; Ayala, P. Y.; Morokuma, K.; Voth, G. A.; Salvador, P.; Dannenberg, J. J.; Zakrzewski, V. G.; Dapprich, S.; Daniels, A. D.; Strain, M. C.; Farkas, O.; Malick, D. K.; Rabuck, A. D.; Raghavachari, K.; Foresman, J. B.; Ortiz, J. V.; Cui, Q.; Baboul, A. G.; Clifford, S.; Cioslowski, J.; Stefanov, B.; Liu, G.; Liashenko, A.; Piskorz, P.; Komaromi, I.; Martin, R. L.; Fox, D. J.; Keith, T.; Al-Laham, M. A.; Peng, C. Y.; Nanayakkara, A.; Challacombe, M.; Gill, P. M. W.; Johnson, B.; Chen, W.; Wong, M. W.; Gonzalez, C.; Pople, J. A. *Gaussian 03*, Rev. E.01; Gaussian, Inc.: Wallingford CT, 2004.
(35) Hay, P. J.; Wadt, W. R. *J. Chem. Phys.* **1985**, *82*, 270.
(36) Wadt, W. R.; Hay, P. J. *J. Chem. Phys.* **1985**, *82*, 284.
(37) Hay, P. J.; Wadt, W. R. *J. Chem. Phys.* **1985**, *82*, 299.
(38) Reed, A. E.; Curtiss, L. A.; Weinhold, F. *J. Chem. Phys.* **1985**, *83*, 735.
(39) Reed, A. E.; Curtiss, L. A.; Weinhold, F. *Chem. Rev.* **1988**, *88*, 899.
(40) Fernández, E. M.; Soler, J. M.; Garzón, I. L.; Balbás, L. C. *Phys. Rev. B* **2004**, *70*, 165403.
(41) Idrobo, J. C.; Walkosz, W.; Yip, S. F.; öğüt, S.; Wang, J.; Jellinek, J. *Phys. Rev. B* **2007**, *76*, 205422.
(42) Majumder, C.; Kulshreshtha, S. K. *Phys. Rev. B* **2006**, *73*, 155427.
(43) Torres, M. B.; Fernández, E. M.; Balbás, L. C. *Phys. Rev. B* **2005**, *71*, 155412.
(44) Yuan, D. W.; Wang, Y.; Zeng, Z. *J. Chem. Phys.* **2005**, *122*, 114310.
(45) Zorriasatein, S.; Joshi, K.; Kanhere, D. G. *J. Chem. Phys.* **2008**, *128*, 184314.
(46) Neukermans, S.; Janssens, E.; Tanaka, H.; Silverans, R. E.; Lievens, P. *Phys. Rev. Lett.* **2003**, *90*, 033401.
(47) Liu, X.; Zhao, G. F.; Guo, L. J.; Jing, Q.; Luo, Y. H. *Phys. Rev. A* **2007**, *75*, 063201.

JP908084U